Coordination Chemistry Reviews 253 (2009) 769–778

Contents lists available at ScienceDirect

Coordination Chemistry Reviews

journal homepage: www.elsevier.com/locate/ccr

Review

Cobalamins uncovered by modern electronic structure calculations

Kasper P. Jensen [a,*], Ulf Ryde [b]

[a] Technical University of Denmark, Department of Chemistry, Building 207, DK-2800 Kgs. Lyngby, Denmark
[b] Lund University, Department of Theoretical Chemistry, P.O.B. 124, S-22100 Lund, Sweden

Contents

ARTICLE INFO

Article history:
Received 12 March 2008
Accepted 26 April 2008
Available online 3 May 2008

Keywords:
Cobalamin
DFT
Vitamin B_{12}
Organometallics
Enzymes

ABSTRACT

This review describes how computational methods have contributed to the field of cobalamin chemistry since the start of the new millennium. Cobalamins are cobalt-dependent cofactors that are used for alkyl transfer and radical initiation by several classes of enzymes. Since the entry of modern electronic-structure calculations, in particular density functional methods, the understanding of the molecular mechanism of cobalamins has changed dramatically, going from a dominating view of *trans*-steric strain effects to a much more complex view involving an arsenal of catalytic strategies. Among these are *cis*-steric distortions, electrostatic stabilization of radical products, the realization that nucleotide units can serve as polar handles, and the careful design of the active sites, with polar residues in the radical enzymes and non-polar residues in the transferases. Together, these strategies explain the enigmatic Co–C bond cleavage necessary for catalysis by these enzymes.

1. Introduction

Coenzyme B_{12} is the largest and most complex cofactor in biology. It contains a central cobalt ion forming a bond to an axial carbon ligand, which made it the first discovered [1] organometallic cofactor in nature. The enigmatic occurrence of a Co–C bond and its catalytic implications have intrigued researchers for decades [1].

Coenzyme B_{12} refers to 5′-deoxyadenosylcobalamin (AdoCbl) and contains a tetra-pyrrole ring system, corrin (Fig. 1). Corrin resembles the porphine ligand, which is the basic unit in porphyrins and hemes. However, corrin lacks one of the four methine bridges, and 10 of the peripheral carbon atoms are sp^3-hybridized, which drastically reduces the extent of the conjugated system, compared to porphine. In the center of the corrin ring, a cobalt ion is bound. The various forms of the cofactor differ by the nature of the axial ligand coordinating to cobalt: in orally administered vitamin B_{12}, a cyanide group is bound to cobalt, but this form is hydrolyzed and transformed into one of two biologically active cofactors, AdoCbl and MeCbl, which contain a

* Corresponding author.
E-mail address: kpj@kemi.dtu.dk (K.P. Jensen).

0010-8545/$ – see front matter © 2008 Elsevier B.V. All rights reserved.
doi:10.1016/j.ccr.2008.04.015

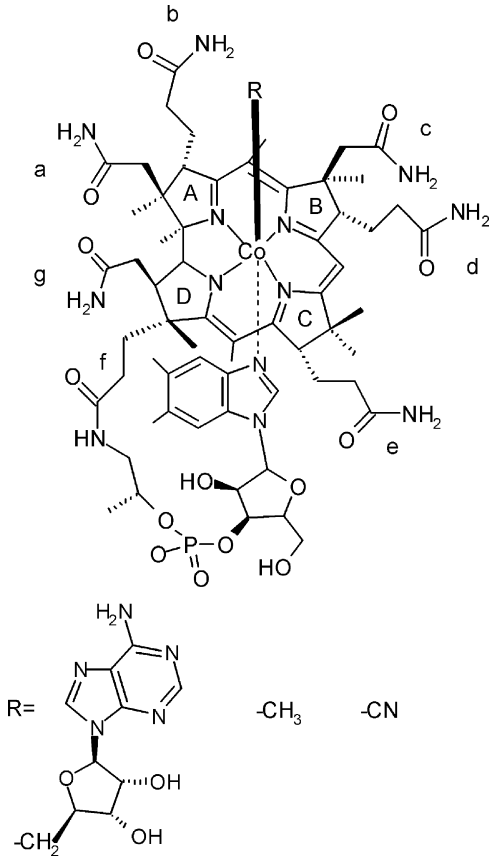

Fig. 1. The cobalamin cofactors with either 5′-deoxyadenosyl (AdoCbl), methyl (MeCbl), or cyanide (Vitamin B_{12}).

5′-deoxyadenosyl (Ado) group or a methyl (Me) group, respectively.

In these resting forms, cobalt is in the Co(III) oxidation state. However, the enzymatic reactions involve also the Co(II) or Co(I) oxidation states, with cobalt always being in the low-spin state [2]. At the periphery of the corrin ring, a number of side chains are bound, mostly methyl, acetamide, and propionamide groups. However, one of the side chains, labeled *f* in Fig. 1, is much longer and ends with a 5,6-dimethyl-benzimidazole (DMB) group, referred to as the nucleotide tail, further adding to the intriguing complexity of the cofactor. In the free coenzyme and also in some enzymes (e.g. the dehydratases) [3], this unusual side chain coordinates back to cobalt via one of the nitrogen atoms of the terminal DMB group. In other enzymes, in particular the human B_{12} enzymes, methionine synthase (MES) [4] and methylmalonyl coenzyme A mutase [5] (MCAM), the nucleotide tail is displaced from cobalt by a histidine amino acid of the protein, a feature that surprised the scientific community and directed a great deal of interest towards the purpose of this axial ligand [6]. In the latter cases, the nucleotide tail is anchored deeply within a protein pocket, providing stability to the protein-bound cofactor.

MeCbl is the cofactor of some transferases, with a role of transferring alkyl cations generated by heterolytic cleavage of the Co–C bond. MES is an example of such an enzyme in humans. The role of MES is to transfer the methyl group of N^5-methyltetrahydrofolate to L-homocysteine to form tetrahydrofolate and L-methionine. L-Methionine may subsequently be converted into *S*-adenosylmethionine (SAM), the central methylation agent used, for e.g. purine, epinephrine, creatine, and melatonin biosynthesis, and thus, inactivation of MES can lead to severe neurological disorders and depression [7].

AdoCbl is used as a cofactor by enzymes such as MCAM, glutamate mutase (GluMut) [8], methyleneglutarate mutase [9], class II ribonucleotide reductase (RNR), ethanolamine ammonia lyase [10], and diol- and glycerol dehydratase [11]. A common feature of these enzymes is that the Co–C bond of AdoCbl is cleaved homolytically, giving rise to a five-coordinate Cob(II)alamin and an Ado radical. The Ado radical subsequently initiates radical-based rearrangements of the substrate, in the case of the mutases (MCAM and GluMut) 1,2-shifts at saturated hydrocarbon centers [12]. MCAM is a metabolic enzyme that converts methylmalonyl coenzyme A, a common product from degradation of various amino acids and lipids, into succinyl coenzyme A, which then enters the citric acid cycle to generate ATP [2].

Understanding why and how AdoCbl and its Co–C bond are used to generate the Ado radical necessary for these reactions constitutes an outstanding problem in bioinorganic chemistry [6], which has recently been answered to a large degree by a combination of experimental and computational chemistry studies. In this context, it is important to appreciate the stability of the Co–C bond in aqueous solution under standard conditions. Homolysis of isolated AdoCbl in aqueous solution occurs very slowly, with rates of $\sim 10^{-9}\,s^{-1}$ at 25 °C [13,14]. The Co–C bond dissociation energy (BDE) has been estimated to be 126 ± 6 kJ/mol [13,15], and the activation enthalpy was found to be ~141 kJ/mol [16], which is larger than the BDE due to thermal and cage effects [17,18]. Thus, this bond is much less stable than a typical organic single bond (the BDE is ~420 kJ/mol for a C–H bond). To be an efficient radical initiator, the enzyme needs to facilitate a controlled and reversible cleavage of the Co–C bond. This problem is complex, and – as we understand it now – has been solved by the evolution of ingenious features in both the coenzyme and enzyme.

Several coenzyme B_{12} dependent enzymes display catalytic rates (k_{cat}) of $\sim 100\,s^{-1}$ [19,20], with the Co–C bond cleavage not even being the rate-limiting step, although possibly rate-limiting when coupled to the hydrogen-abstraction step [20]. Later steps, in particular radical rearrangements, are faster [21]. In MCAM, the homolytic cleavage proceeds with $\Delta G^{\ddagger} = 55 \pm 3$ kJ/mol and $\Delta H^{\ddagger} = 79 \pm 4$ kJ/mol at 37 °C [22]. Thus, MCAM and GluMut accelerate Co–C bond homolysis by as much as 12 orders of magnitude [20], and lower $\Delta G^{\ddagger}$ by up to 70 kJ/mol. Importantly, the enzymes shift the equilibrium constant towards the homolysis products by a factor of 3×10^{12} (74 kJ/mol), giving an equilibrium constant close to unity [16,23]. This makes the reaction reversible and allows the reformation of the 6-coordinate Co(III) resting state at the end of the reaction cycle. The causes of these large catalytic effects and the nature of this ingenious radical initiation–termination mechanism have been much discussed, and until recently remained a major unsolved problem of bioinorganic chemistry.

In this account, we will shortly discuss the status of the issue prior to the new millennium, with the confusion caused by the publication of several crystal structures of B_{12}-dependent enzymes, and then turn to recent progress facilitated by computational chemistry, and summarize the current view of the strategies employed by cobalamin-dependent enzymes. The focus will be on results obtained from computational chemistry, particular within our own group, but with a careful account of the interplay between these studies and the works of other computational and experimental groups.

2. Early emphasis on *trans* effects

Decades ago, several different mechanisms were suggested for coenzyme B_{12}-dependent enzymes. Much of this early work was based on studies of cobaloximes [24], i.e. R-L-bis(dmgH)cobalt complexes (where dmgH = the monoanion of dimethyl glyoxime),

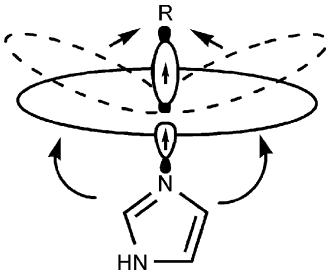

Fig. 2. The steric and electronic *trans* effects envisioned in cobalamins to explain Co–C bond weakening.

which were used extensively as cobalamin model systems [25,26]. Early research focused on *trans*-electronic and *trans*-steric effects as known from classical coordination chemistry [27–29], and it was tempting to put emphasis on the flexibility of the bis(dmgH) ligand, indirectly interpolating this flexibility to corrins [30]. Two notions arose from the cobaloxime studies: (i) a strong nucleophilic axial N-ligand could reduce the strength of the *trans* axial Co–C bond by *trans*-electronic effects, in particular by increasing the electron density on cobalt and in the anti-bonding σ-orbital of the Co–C bond and (ii) a bulky N-ligand could clash with and cause upwards "butterfly" folding of the dmgH (or by analogy, corrin) ligand, thereby elongating and weakening the Co–C bond [31–33]. These mechanisms were subsequently referred to as *mechano-chemical labilization* [32] and are depicted schematically in Fig. 2.

However, the electronic structure of the tetradentate corrin ring is quite distinct from the two bidentate bis(dmgH) ligands, as semi-empirical computations and crystal structural studies of both kinds of model complexes have shown [34–36]. In particular, the cobaloxime charge and electron density on cobalt differ from those of corrins, mainly because bis(dmgH) is a dianionic ligand, whereas corrin is mono-anionic. This causes differences in electrochemistry and reduces the usefulness of the cobaloxime model, as was early noted [37]. It is thus clear that the suitability of the cobaloximes as cobalamin models has been overestimated.

A series of molecular-mechanics (MM) studies of the conformations of cobalamins provided the first detailed insight into the nature of corrin conformations [38]. However, whereas many of these results, e.g. relative energies of cobalamin conformations, were quite useful, the significance of *trans* effects on the Co–C cleavage problem cannot be studied by classical methods since the description of the actual Co–C bond cleavage reaction requires electronic-structure methods.

Thus, there was an early anticipation that a major part of the catalytic effect of cobalamin-dependent enzymes had to derive from structural changes in the corrin framework, more precisely from a shortening of the Co–N_{ax} bond, which, according to the mechano-chemical mechanism, would labilize the Co–C bond by *trans*-electronic or *trans*-steric effects, as seen in Fig. 2. This ensured that the focus remained on the corrin part of the cofactor [33]. However, a variety of other suggestions of catalytic strategies have been put forward, including specific interactions involving the corrin and its side chains [12,16], twisting of the axial Co–N_{ax} bond [39], tilting or pulling the Ado group [40,41], or the protein favoring the dissociated state more than the resting state [42,43].

At this stage, emerging crystal structures of B_{12}-dependent enzymes [5,4,44] indicated that there is no significant structural distortion of the corrin moiety in the substrate-free enzymes [45]. In particular, the so-called corrin fold angle, which is a structural measure of the degree of distortion of the corrin ring away from planarity [2], was smaller in proteins than in solution [46], i.e. the cobalamins were less upward-folded in the proteins than in solution. Furthermore, most crystal structures of coenzyme B_{12} enzymes revealed Co–N_{ax} bonds that were in fact longer, rather than shorter, than for the isolated coenzyme [46]. Thus, there was no indication of any mechano-chemical labilization from the crystal structures. On the other hand, crystal structures with substrates invariably displayed broken Co–C bonds [47,48], which indicated that substrate-induced conformational changes may trigger Co–C bond cleavage in some way.

Owing to these structural data, it was subsequently suggested that a *lengthening* of the Co–N_{ax} bond could selectively stabilize the Co(II) oxidation state [5,49]. This suggestion is hard to reconcile, in particular since the Co(II) state has a slightly shorter Co–N_{ax} bond than the Co(III) state [50]. Any lengthening of this bond would have the opposite effect of actually strengthening the Co–C bond, which is indeed observed experimentally: for example, base-off AdoCbl has a BDE of 144 kJ/mol, which is 18 kJ/mol more than the base-on form [51]. Any elongation of the Co–N_{ax} bond length would thus in fact increase the Co–C BDE. Quite soon thereafter, refined EXAFS data [52] showed that GluMut and 2-methylenglutarate mutase have Co–N_{ax} bonds of 2.1–2.2 Å, which agrees with what is found for the isolated cofactors [2]. Likewise, EPR studies of five B_{12}-dependent enzymes indicated similar bond lengths [53]. Finally, mutations of either the axially coordinating His or its hydrogen-bond partner Asp in GluMut leads to a 1000-fold decrease in k_{cat} [54], which sets an upper bound to the importance of the axial N-ligand in the enzymes and is comparable to its ∼100-fold effect on Co–C cleavage in the isolated cobalamins [51]. Thus, it became clear that the importance of the Co–N_{ax} bond in modulating the enzymatic reaction had been grossly overestimated.

Incidentally, as data mounted against any involvement of the axial His in weakening the Co–C bond, other roles of this ligand were suggested. One was to prevent the unwanted side-reaction of heterolysis in mutases [55], whereas another would be to provide structural stability and specificity to the cobalamin binding site [56–58].

3. Computational studies of corrin models

3.1. B3LYP studies of corrin models

With the advent of efficient computer algorithms and fast computers, quantum mechanical computations of structure, energies, and other properties have reached an accuracy comparable to or sometimes even surpassing that of experimental data, e.g. for geometries of metal sites in low- and medium-resolution crystal structures of proteins [59]. The first theoretical studies of cobalamin chemistry were pursued on simplified corrin models [60], and then on full corrin models with simplified semi-empirical quantum-mechanical methods [34]. Semi-empirical methods can provide reasonable optimized structures and give a good picture of the suitability of various types of model systems by comparing bond lengths and angles [34,35]. However, current semi-empirical methods are insufficient for studying almost any other property of metalloproteins, except if parameterized specifically for the problem [61].

At the beginning of this millennium, several groups began to apply density functional theory (DFT) to the study of cobalamins. While studies of the radical reactions subsequent to Co–C bond cleavage had been pursued separately [62–65], these new approaches used full corrin models of cobalamins to gain insight into the fundamental Co–C cleavage problem [46,66–92].

The first of these studies used the B3LYP functional [93], which had a proven excellent performance for main group elements [94] and had successfully worked for other types of radical enzymes [95]. Experience had shown that many properties, including structures, frequencies, and some types of energies, are accurately

described by B3LYP even for transition metals [96,97], and part of this success was witnessed already with the generalized gradient approximation (GGA) functionals [98–100], such as the widely used BP86 functional [101,102].

However, these functionals are less successful when studying energy differences between qualitatively different electronic configurations [103,104], e.g. configurations with different numbers of unpaired electrons. B3LYP, being a hybrid functional with some amount of Hartree–Fock exchange energy included, favors open-shell configurations and high-spin states more than non-hybrid functionals such as BP86 [105]. This difference turns out to be exceedingly important in cobalamin chemistry, where the Co–C bond cleavage generates two molecules with open shells that are described quite differently by different functionals [66].

The first B3LYP studies [66,68,69] dealt with the structural correlations between axial ligands in corrin models, in particular *trans*-steric and *trans*-electronic influences of the axial N-ligand on the Co–C bond length, and thus indirectly on the Co–C bond strength. These studies gave excellent structures, with all bond lengths within 0.02–0.05 Å of experiments, except the Co–N_{ax} bond lengths, which were ∼0.3 Å too long [66,68]. The reason for this is that the Co–N_{ax} bond is extremely flexible: its length can be varied over a range of 0.5 Å at an energy cost of less than 3 kJ/mol [46], quantifying the suggested "substantial energy cost" [106] of variations in this bond. The Co–C bond turned out to be ∼5 times stronger than the Co–N_{ax} bond. Therefore, the N-ligand cannot weaken the Co–C bond (but the Co–C bond has a strong *trans* influence on the Co–N_{ax} bond). This observation was in stark contrast to observations of *trans* effects in cobaloximes and indicated that conclusions drawn from cobaloxime chemistry had been overemphasized.

These structural correlations were further substantiated by B3LYP calculations of the actual Co–C bond strengths [70,74]. The Co–C bond strength is computed from Eq. (1), which defines the homolytic bond dissociation energy (BDE):

$$\mathrm{BDE} = E[\mathrm{Co(II)}] + E[\mathrm{R^{\bullet}}] - E[\mathrm{Co(III)R}] \quad (1)$$

Here, E[Co(II)] is the computed quantum-mechanical energy of the fully geometry-optimized Cob(II)alamin model, E[R•] is the corresponding energy for the radical fragment, and E[Co(III)] is the energy of the cob(III)alamin resting state with the R ligand bound to cobalt. These energies can be converted into computed bond dissociation enthalpies by adding zero-point and thermal effects.

The BDEs computed in this way directly showed that the Co–N_{ax} bond length has a small effect on the Co–C bond strength. This was true for the natural N-ligands imidazole (a model of the His ligand in proteins) and DMB [46,70], as well as for a deprotonated imidazole ligand [46], which might form in the enzymes upon deprotonation of the His by the adjacent Asp residue. In fact, a maximum contribution of 15 kJ/mol from the axial N-ligand was estimated [46].

At the same time, other properties, such as absorption spectra [72,75] and kinetic isotope effects [73] were calculated for realistic corrin models with B3LYP, providing additional insight into the nature of excited electronic states and the feasibility of coupled Co–C cleavage and hydrogen abstraction. Errors in DFT-computed excitation energies can be quite large, and in the cobalamin studies, the average errors were 0.2 eV [75] and 0.5 eV [72], the latter errors probably being due to the basis set lacking diffuse functions and polarization functions on cobalt.

3.2. Changing the density functional

A major problem with the B3LYP calculations was that the Co–C BDEs were underestimated by 35–80 kJ/mol [74]. This cast doubt on the ability of DFT to model this crucial descriptor of the Co–C bond cleavage problem. A turning point in the computational work occurred with a detailed investigation of metal–carbon BDEs in B_{12}-like systems, in which energies were obtained from a variety of methods, corrected by zero-point energies, thermal corrections, relativistic effects, basis set effects, solvent effects, and counterpoise corrections [66]. It was shown that the main reason for earlier failures to compute the Co–C BDE resided in the functional B3LYP, due to a bias of the exact Hartree–Fock exchange (and to some extent the LYP correlation functional) towards the homolysis fragments [66].

It is now known that hybrid functionals, such as B3LYP, tend to underestimate BDEs of bonds between transition metals and ligands, whereas pure GGA functionals, such as BP86, tend to overestimate them [105]. In simple transition-metal complexes, these systematic errors are of a similar magnitude (but with opposite signs), giving similar average errors for the two types of functionals [105]. However, in the case of organometallic systems, B3LYP drastically underestimates the BDEs, whereas GGA functionals perform well. The main reason for this discrepancy is that most simple transition-metal complexes are in the high-spin state before cleavage [105]. This means that the B3LYP bias towards the dissociated state is smaller, and more reasonable energies are obtained for the high-spin complexes. However, the Co(III) state of cobalamins is closed-shell and low-spin and therefore the bias towards the dissociated state becomes too large [66].

Because of these effects, it was found that non-hybrid functionals performed much better than B3LYP for a variety of organometallic systems [66]. In particular BP86 turned out to perform consistently well for many related types of systems, i.e. octahedral organometallic systems, with errors of ∼10 kJ/mol (compared to the 35–80 kJ/mol errors from B3LYP). The good performance of BP86 has been noticed in other aspects of transition metal chemistry as well [107].

Interestingly, the geometric differences between structures optimized with different functionals were small, and almost all of the B3LYP BDE error remained also when computing energies at the BP86-optimized geometries [66], so the pronounced differences are due to inherent differences in the treatment of the electronic configurations at *any* geometry. The results discussed above have led to that almost all later computational work in the field has been carried out with the BP86 functional, and the results have been verified independently later [87].

The application of proper methodology to the study of cobalamin chemistry has also been an issue in relation to reductive cleavage of cobalamins [108,109]. The B3LYP method was used to study such reactions, where an electron relocates from a corrin-based π^* to a Co–C bond-centered σ^* orbital [108]. The fact that B3LYP showed a negligible change in Co–C bond length upon reduction was taken to imply that DFT as a whole is inappropriate for modeling cobalamin chemistry [108], which was earlier disproved based on explainable differences between hybrid and non-hybrid functionals [66]. A subsequent CASSCF study of the cleavage reaction provided an interesting comparison to B3LYP [109]. However, CASSCF alone does not include dynamical correlation outside the active space and suffers from some of the core-valence correlation problems of HF; in addition the choice of active space needs to be carefully calibrated and chemically reasonable. It is clear that non-dynamical correlation effects are introduced upon Co–C bond cleavage, but although the CASSCF approach can provide important qualitative information, only non-hybrid functionals so far have stood the test against experimentally determined BDEs. There is still controversy regarding the mechanism of reductive cleavage of cobalamins, although the most reliable method currently available, BP86, can explain the observed activation enthalpy of reductive cleavage quite well [87,110].

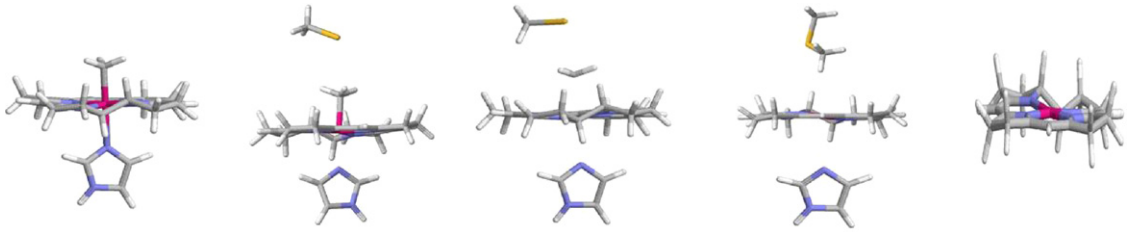

Fig. 3. Optimized geometries of intermediates in the methionine synthase reaction [78] from left to right: separated reactants, reactant complex, transition state, product complex, and separated products. Reproduced with permission from ref. [78]. Copyright 2003 Am. Chem. Soc.

3.3. Studying the methionine synthase reaction

The first study of a cobalamin-dependent enzymatic reaction including a corrin model was carried out on MES, using the B3LYP method [78]. In this case, the bond cleavage is heterolytic, with all reaction species remaining closed-shell throughout the reaction. Therefore, various functionals give similar results [66], so the conclusions drawn from this study remain valid.

Reaction and product complexes, and the transition state for the homocysteine nucleophilic attack on MeCbl were fully optimized, as shown in Fig. 3. The results indicated the importance of a non-polar protein environment in facilitating nucleophilic attack by homocysteinate on MeCbl, explaining the presence of hydrophobic residues around the methyl group in MES [4]. Moreover, the need for the deprotonation of homocysteine was clearly demonstrated [78]. Since heterolytic cleavage in the transferases is a highly polar reaction, with a positive charge being transferred from cobalamin to the methyl cation acceptor, the axial N-ligand has a larger influence on these reactions [79]. One important role appears to be to avoid the formation of the unwanted Cob(II)alamin [111]. Another possible role, which remains to be tested, is that there is a lower energy cost of dissociating His than DMB in the protein, due to the tighter binding of DMB via the nucleotide tail (the N-ligand dissociates during the MES reaction [112]).

The generation of and control over the strong nucleophile Cob(I)alamin, the catalytic challenges and possibilities that such a specialized reducing agent implies, and the accessibility of the unusual Co(I) oxidation state, are issues that have attracted some interest from computational groups [77,86,113]. It was found that the B3LYP functional locates a singlet instability for the electronic structure of Co(I)corrin [77], providing an open-shell singlet ground state, 4 kJ/mol lower than the closed-shell singlet. This would suggest that Cob(I)corrin has a multi-configurational ground state involving other configurations than the d^8 Co(I) configuration. These results were later confirmed by accurate multi-configurational *ab initio* (CASPT2) calculations of Co(I)corrin [113], implying that the wave function of Co(I)corrin consists of up to 23% open-shell configurations.

If Cob(I)alamin already contains some degree of Co(II)Cor^{2-} configurations, it may explain the accessibility of this supernucleophile [113]. In this sense, the cob(I)alamin cofactor resembles compound I in heme peroxidases and cytochrome P450, with a non-innocent tetrapyrrole ring (see Fig. 4), but with an opposite direction of the charge transfer. This illustrates a convergent molecular evolution towards energetically close-lying ligand and metal orbitals, tuned to provide access to unusual oxidation states.

Spectroscopic studies have been performed in great detail on cob(I)alamin [86], and a closed-shell ground state sufficed to explain qualitatively the spectroscopic data. However, as shown in the *ab initio* study [113], CASPT2, which treats all configurations of the ground state in a balanced manner, accounts better for the experimental ligand-field spectrum. Furthermore, recent alternative reaction mechanisms involving radical nature in the activated state of MES have been suggested [88]. These studies revealed a partial radical nature of the Co(I)corrin moiety, consistent with the CASPT2 results.

3.4. Studies of Co–C cleavage in the mutases

3.4.1. Effects of the protein

Until now, we have discussed only computational studies of models involving the cobalamin cofactors themselves. However, as we have seen, the experimentally reported labilization of the Co–C bond was not consistent with any distortions or electrostatic effects that could simply be forced upon the cobalamin moiety. Thus, attention turned towards the role of the protein in weakening the Co–C bond. Perhaps the architecture of the cobalamin cofactors is only important for providing a Co–C bond with a low homolytic BDE, whereas further lowering of this BDE is achieved by the protein.

A first insight into the Co–C bond cleavage problem came from computational work that included a few of the residues surrounding the Ado group in MCAM [80]. Although this work was performed with B3LYP, and thus the Co–C BDE was substantially underestimated, the general effect of these amino acid residues on the Co–C dissociation curve appear to be valid [84]. This work pointed

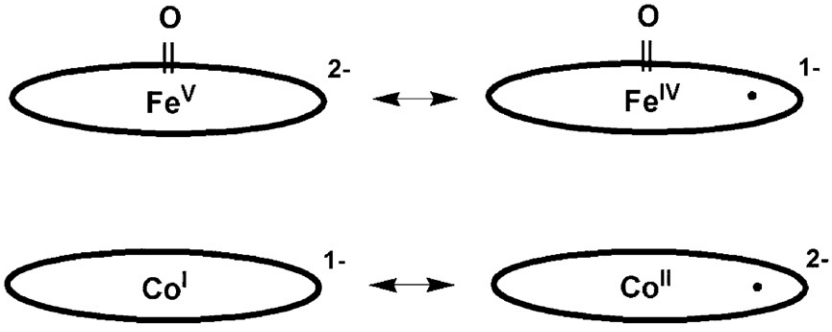

Fig. 4. Resonance forms contributing to the stability of extreme oxidation states in tetrapyrroles.

towards the importance of hydrogen bonds stabilizing the Ado radical and that Ado does not fully from dissociate from Co in the protein, with a total lowering of the BDE by 51 kJ/mol for a minimal model of the protein including three residues [80]. Along similar lines, it was explained why the solution Co–C BDE of AdoCbl is ca. 20 kJ/mol smaller than that of MeCbl [114]. This required a more careful computational study of the models in solution, showing that intrinsic steric and electronic effects also reflected in the 0.03 Å longer Co–C bond weakens the AdoCbl Co–C by ca. 20 kJ/mol relative to that of MeCbl [114]. In vacuum, it was found that there is a strong stabilization of AdoCbl due to van der Waals interactions, which are also present in the studies of MCAM and in the protein, counteracting the steric and electronic destabilization. However, this effect is screened in solution, explaining why a difference is observed in experimental studies of the isolated cofactors [114].

3.4.2. QM/MM studies of mutases

The next natural step was therefore to include the protein in the computational studies. The first example of such an approach was a combined quantum-mechanical and molecular-mechanical (QM/MM) study of MCAM [81], using the B3LYP functional and the Amber force field [115,116]. This study showed that the essential conclusions drawn from isolated cobalamin models remained valid also in the protein [81]. There were still no *trans*-electronic or *trans*-steric effects mediated via the corrin framework upon Co–C cleavage. These results were in good agreement with Raman spectroscopic data for MCAM, indicating no structural change in the corrin ring upon Co–C bond labilization in this protein [40].

Soon after, a comprehensive QM/MM study of GluMut was presented [84], which used BP86 as the density functional and Amber as the force field, with special parameters for cobalamin [117]. This study presented QM/MM computations of the Co–C bond cleavage in GluMut using the ComQum software [118,119]. GluMut structures were chosen because they represented the most accurate and non-ambiguous available crystal structures of B_{12}-dependent enzymes [47,48]. In contrast, the corresponding MCAM structure [120] displayed a questionable geometry of the Ado group [121].

A recent structure of GluMut crystallized with glutamate was used as starting point for the QM/MM computations. This structure displays two conformations of Ado with similar populations, one 3.2 Å from Co and the other 4.5 Å from Co (thus, the Co–C bond is broken in both conformations) [48]. GluMut resembles MCAM in function and class: both are mutases that perform 1,2-shifts at saturated carbon centers. GluMut consists of two subunits, MutE and MutS [54]. MutS shares with MCAM and MES the Asp-*X*-His-*X*-*X*-Gly motif, which is a fingerprint of His binding to cobalt [122]. The MutE subunit has no apparent similarity with other B_{12}-dependent enzymes and seems to contain the specific substrate-binding site [54]. The enzymatic reaction is the stereospecific conversion of (*S*)-glutamate to (2*S*,3*S*)-3-methylaspartate [123].

Our study [84] showed that GluMut reduces the Co–C BDE of AdoCbl from 143 kJ/mol in vacuum to 8 kJ/mol in the protein. The calculations also allowed us to identify four important sources to this large effect: first, 20 kJ/mol comes from the fact that the Ado radical never completely dissociates from the enzyme, confirming the small-model calculations [80]. Second, the surrounding enzyme stabilizes the dissociated state by 42 kJ/mol, using mainly electrostatic interactions. Third, the enzyme itself is stabilized by 11 kJ/mol in the dissociated state. Fourth, the coenzyme is distorted by the surrounding enzyme, and this distortion is 61 kJ/mol larger in the Co(III) state than in the Co(II) state.

These factors could be further decomposed into contributions from the various residues in the enzyme or the parts of the coenzyme. For example, the direct electrostatic effect is dominated by contributions from Arg-66, Lys-326, and the substrate, which all interact with the ribose moiety of the coenzyme, and Asp-14, which is the residue that forms a hydrogen bond to the axial His ligand. Moreover, we showed that the distortion of the coenzyme is caused almost entirely by van der Waals interactions and not by electrostatics. *In silico* mutations showed that Lys-326, Glu-330, a side-chain of the coenzyme, and the substrate were most responsible for this effect, but several other residues also contributed in a cooperative manner. All these residues are close to the Ado part of the coenzyme, showing that it is mainly this part that is affected by the enzyme (Fig. 5).

This was confirmed by direct calculations of the strain energy in the various part of the coenzyme: the His and corrin moieties were hardly strained at all, whereas the adenine and especially the ribose moieties were strongly destabilized. The largest effect was seen for the Co–C5′–C4′ angle (38 kJ/mol). This was also confirmed by the corresponding QM/MM optimizations of MeCbl and ribosylcobalamin in the enzyme, which showed much smaller catalytic effects (42 and 109 kJ/mol, compared to 135 kJ/mol for AdoCbl). This directly explains why MeCbl cannot be used in the homolytic cobalamin-dependent enzymes: it simply lacks the polar handle (the adenine and in particular ribose groups) that is needed to disfavor the Co(III) state by both direct electrostatic and indirect (through a geometry change) van der Waals interactions.

A subsequent work [92] used the same methodology (BP86/Amber) with the ONIOM QM/MM approach, to study Co–C bond cleavage in MCAM. This provides an interesting comparison between the two proteins, which are expected to have similar catalytic strategies. Both studies indicated a significant reduction of the Co–C BDE to 8–10 kJ/mol in the enzymes. However, in GluMut, a single-step mechanism without any transition state was observed, whereas for MCAM, a transition state for Co–C bond cleavage was found at a Co–C distance of 2.67 Å and an energy of 42 kJ/mol above the Co(III) state [92]. This transition state was not directly connected to the Co(III) state. Instead, an intermediate was found with a Co–C bond length of 2.17 Å, a very long Co–N_{ax} bond length of 2.9 Å, and an energy of 29 kJ/mol. It differed from the true Co(III) state in the conformation of the Ado group and this difference was also connected to differences in the conformation of the substrate. In fact, the substrate-free enzyme exhibited a 40 kJ/mol smaller catalytic effect, and the open form of the enzyme gave no catalytic effect at all. Unfortunately, no connection between the Co(III) state and the intermediate was found and no attempt was made to decompose and understand the observed energetic effects.

3.4.3. The empirical valence bond approach to B_{12}

Another study [90] used the empirical valence bond (EVB) methodology [124,125] to study the Co–C homolysis in MCAM. This approach allows for an enlightening comparison to the QM/MM studies [84]. Both methods have their strengths and weaknesses: the QM/MM studies used BP86 calculations along the Co–C bond dissociation curve, which are known to be in good agreement with experiment and account well for the electron correlation effects involved [66]. However, the computational cost of these calculations does not allow for conformational sampling, which means that entropy is ignored and there is a risk to end up in artificial local minima (but this risk is reduced by running the calculations forth and back until the potential energy curve is smooth and reproducible [84]). On the other hand, the EVB method employs a much faster but less accurate MM force field, and this allows for sampling of phase space. Therefore, free-energy perturbations can be performed, giving free energies and an estimate of entropy effects. The disadvantage is that the potential energy surface used for the Co–C bond cleavage is calibrated based on DFT and empirical data and thus loses parts of its predictive nature. The use of B3LYP cal-

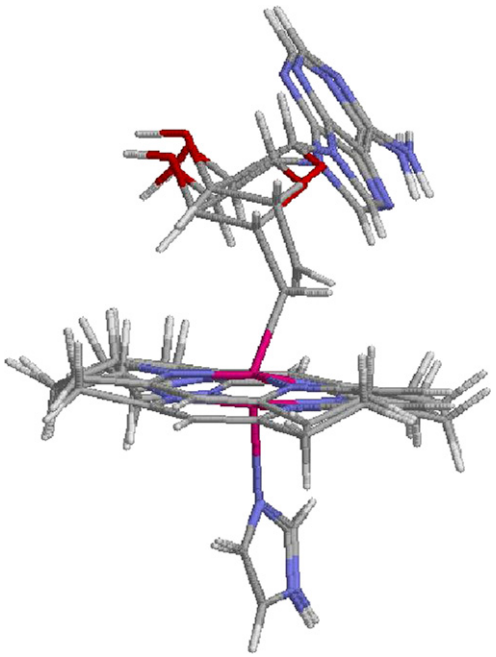

Fig. 5. Comparison of the QM/MM-optimized Co(III) and Co(II) states in glutamate mutase, showing a negligible corrin deformation upon Co–C bond cleavage [84]. Reproduced with permission from ref. [84]. Copyright 2005 Am. Chem. Soc.

culations for the calibration is also a drawback of the EVB study, as explained earlier. Finally, another difference is that the EVB study used the corresponding reaction in aqueous solution, rather than in vacuum, as the reference.

The EVB calculations gave a 67 kJ/mol lowering of the free energy of Co–C bond cleavage in MCAM [90]. No transition state was found, in agreement with the GluMut study [84], but in contrast to the QM/MM study on MCAM [92]. In fact, it was argued that the transition state and the intermediate found in the QM/MM study are artifacts of the energy minimization [90]. Interestingly, if the same Co–C bond cleavage process was studied with the point charges of the coenzyme removed, the catalytic effect completely disappeared, indicating that it is essentially electrostatic in nature [90]. This is in stark contrast to the GluMut investigation, in which most of the catalytic effect remained (111 kJ/mol) even if all the protein charges were zeroed [84]. The catalytic effect could be attributed mainly to the better solvation of the ribose and adenine parts of the coenzyme in the protein than in water solution, and the hydrogen bonds between ribose and Glu-370 (corresponding to Glu-330 in GluMut) was pointed out as the main source of this stabilization, although the suggestion was not quantified [90]. Thus, the study confirms the important conclusion of the GluMut study that the Co–C homolysis is accomplished by employing the ribose group as a polar handle [84].

Finally, the EVB study gave a reaction free energy for the Co–C bond homolysis of 54 kJ/mol in MCAM [90], in contrast to the experimental observation of an equilibrium constant close to unity [16,23]. However, this discrepancy was corrected if the radical transfer to the substrate was also considered (giving a reaction free energy of 13 kJ/mol), indicating that the two reaction steps are concerted [90]. In GluMut, this effect was smaller, only 16 kJ/mol [84].

4. What makes cobalamins special, compared to other tetrapyrroles?

4.1. Proof of thermodynamic preferences for evolved metal-ligand combinations

Cobalamins are structurally related to other tetrapyrroles employed in nature, such as heme, coenzyme F430, and chlorophyll. All these tetrapyrroles have their distinct metals (Co, Fe, Ni, and Mg, respectively) and functions. A study of the correlation between structure and function of tetrapyrrole cofactors is instructive for understanding the molecular evolution, and in the context of cobalamins, it is interesting to understand what makes these cofactors more suitable than other tetrapyrroles for carrying out the type of chemistry that we have discussed in the previous sections.

Fig. 6 shows the porphine, corrin, and hydrocorphin frameworks of hemes, cobalamins, and cofactor F430, respectively. An interesting question, not only from a molecular-evolution perspective, but also from the viewpoint of designing catalysts, is to what extent the differing functions are caused by the tetrapyrrole ligands, the metal ions, or the surrounding proteins. Such questions are hard to answer by experimental methods, but they are well suited for quantum mechanical calculations, which can be used to compare the intrinsic properties of the isolated cofactors, without any effects of the individual proteins [77,85].

Density functional theory has been used to study modified tetrapyrrole ring systems, to better understand these issues [77,85]. The functionals used were again BP86 and B3LYP, and the general strategy was to study not only the native types of tetrapyrrole–metal complexes, but also other combinations of ligands and metals, with a variety of axial ligands attached. Such studies could explain why nature needs highly specialized ligand systems such as the tetrapyrroles, and why particular metal ions were used for each of them.

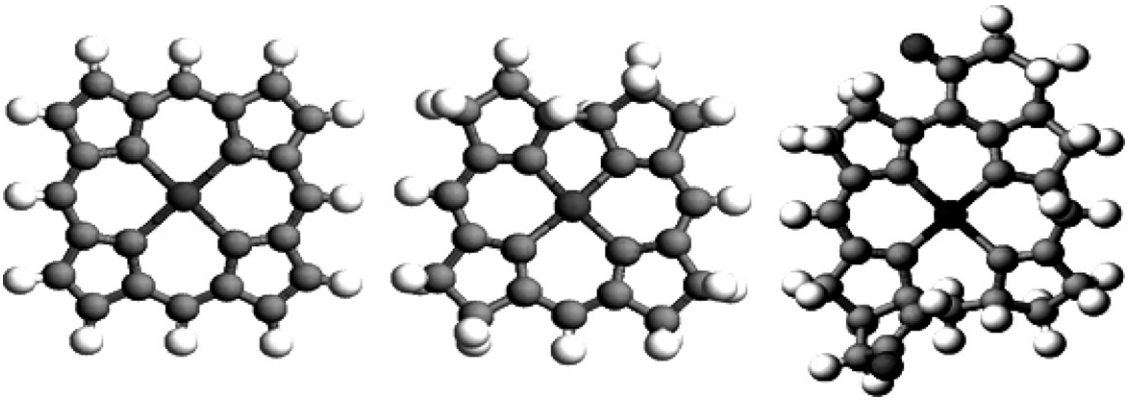

Fig. 6. Examples of basic ring systems of tetrapyrrole cofactors in biology: porphine (left), corrin (center), and hydrocorphin (right).

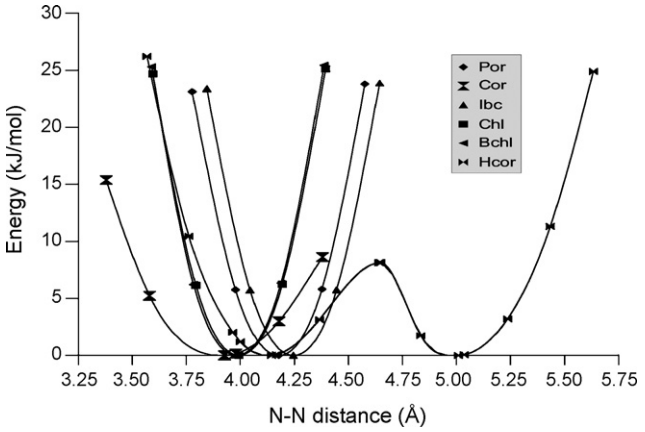

Fig. 7. Potential-energy curves for distortion of the cavities in corrin (Cor), porphyrin (Por), chlorin (Chl), hydrocorphin (Hcor), bacteriochlorin (BChl), and isobacteriochlorin (Ibc). Reproduced with permission from ref. [86]. Copyright 2005 Society of Porphyrins and Phtalocyanines.

A first thing investigated was the importance of the size of the central cavity of each tetrapyrrole ligand in determining the selectivity between metal ions [126]. Fig. 7 shows the cavity size from DFT-optimized geometries of tetrapyrrole rings without metal ions bound (the minima of the curves), as well as the flexibility of the ligands in terms of energy required to distort oppositely located nitrogen atoms. The calculations were carried out for corrin (Cor), porphyrin (Por), hydrocorphin (Hcor), chlorin (Chl), bacteriochlorin (Bchl), and isobacteriochlorin (Ibc) [85]. It can be seen that the flexibility of the rings follows the trend Hcor > Cor > Por ∼ Ibc > Chl > Bchl, showing that corrin is more flexible than porphine, but less flexible than hydrocorphin. On the other hand, the cavity sizes follow the order Cor < Bchl ∼ Chl < Por < Ibc < Hcor. These trends can be compared to the (octahedral) ionic radii of the various ions: LS Co^{III} ∼ LS Fe^{III} < LS Ni^{III} < HS Ni^{III} < HS Co^{III} ∼ LS Fe^{II} < HS Fe^{III} ∼ LS Co^{II} < HS Ni^{II} < Mg^{2+} < HS Co^{II} < HS Fe^{II} (LS = low-spin, HS = high-spin) [127]. This comparison directly explains the preference for low-spin cobalt in the cobalamins and why higher spin states are allowed in hemes. This result is profound, as it outlines a correlation between electronic structure and function, which goes all the way to the proteins: heme-dependent proteins can utilize close-lying spin states to bind small ligand and activate them [128,129], whereas cobalamin-dependent proteins maintain low-spin chemistry with directed σ-orbitals necessary for reversible radical formation; the presence of higher spin states would slow down reformation of radicals since spins would need to flip during reaction, something which, on the other hand, is essential in the O_2-activating heme enzymes.

The small cavity of corrin is also reflected in optimized models of metal tetrapyrroles, in which the equatorial M–N bonds are ∼0.09 and ∼0.20 Å shorter in Cor than in Por or Hcor, respectively, independently of the metal. The reason for this is that corrin lacks one of the bridging methine groups (cf. Fig. 6) [85].

A problem with this study is that the ionic radii of the metals depend on the axial ligands and the type and charge of the equatorial ligands, i.e. that the conclusions of metal ion selectivity and spin preferences may not be valid in the various proteins with different axial ligands. To meet such criticism, the ideal sizes of the various ring systems were probed by computing the geometries of ring-broken models of the tetrapyrroles, such as those shown in Fig. 8 [77,85]. These models retain the charge, the number of bonds in the chelating rings, and the conjugation of the real tetrapyrroles, but they cannot enforce suboptimal M–N distances (M is the metal) by covalent strain within the ring systems, and will thus probe the ideal values of these bonds.

Calculations with these models showed that the cavity in corrin indeed is ideal for low-spin Co(I), Co(II), and Co(III), because the Co–N bond lengths are the same in the normal and ring-broken models within 0.03 Å [77,85]. Thus, it is not surprising that the corrin ring can incorporate the Co(I) ion. On the other hand, the central cavities in Por and Hcor are too large for all metal ions in their low-spin states. Thus, Hcor is ideal for incorporating the large high-spin Ni(II) ion, whereas the Por ring renders also the higher spin states of Fe accessible. The results are also directly reflected in calculated energy splittings between low-spin and high-spin states, which are much larger for Co than for Fe, an effect that can be attributed both to the metal (∼40 kJ/mol) and to the tetrapyrrole (∼50 kJ/mol) [77]. Thus, both the choice of metal ion and ligand framework contribute to the different functionalities implied by the various spin regimes.

Another test of the intrinsic preferences of the various tetrapyrrole ring systems for the particular metal ions is to directly exchange metal ions between the various ring systems, i.e. to study substitution reactions of the type CoCor + FePor ↔ CoPor + FeCor. It was found that for nearly all oxidation states and combinations of axial ligands, the native combinations, i.e. CoCor, FePor, and NiHcor, were thermodynamically favored [77,85]. This shows that the biological tetrapyrrole cofactors were co-evolved as functional units to fit together one particular metal ion and ring system.

4.2. Functional advantages of metal and ligand combinations

The next logical step was to look in detail at the functionality accompanying these units. For example, a typical function of heme in cytochromes is electron transfer. It was shown that heme with low-spin Fe(II) and Fe(III) is ideally suited for electron transfer, because the structural differences between these two oxidation states (with two neutral axial ligands) are minimal, leading to a very small inner-sphere reorganization energy (∼8 kJ/mol) [130], and therefore a high rate for electron transfer. This is an effect of the metal ion, because nearly the same reorganization energy was obtained for Fe(II/III)Cor. On the other hand, the Co(II/III) couple is not suited for electron transfer: both CoPor and CoCor exhibit very high reorganization energies (179 and 197 kJ/mol) [77]. The reason is that Co(II) has seven 3d electrons, and therefore, in variance

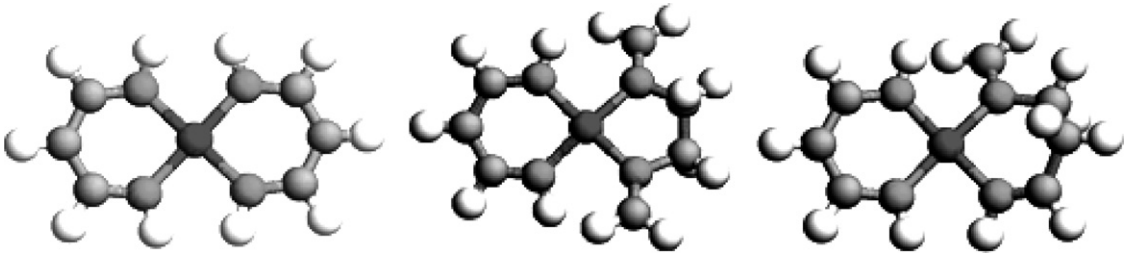

Fig. 8. The three models used to estimate ring strain in Por, Cor, and Hcor, respectively [77,85].

to Co(III), Fe(II), and Fe(III), has an occupied $3d_{z^2}$ orbital, directed towards the axial ligands. This results in a major weakening of the axial bonds in the Co(II) state and therefore leads to a large reorganization energy. Consequently, theory can explain why iron is a natural choice for electron transfer. This has later been confirmed also from computational studies of metal-substituted iron–sulfur clusters [131].

Equally interesting are the reduction potentials of the various tetrapyrrole complexes. The ring system has a pronounced effect on the potential of the metal ion: in water solution, the potential of Fe is lower than that of Co, e.g. +0.77 V for the Fe(II/III) couple, compared to +1.82 V for Co(II/III) [132]. However, in the tetrapyrroles, the reduction potential of Fe is 0.2–0.5 V *higher* than that of Co (and that of Ni is ~0.2 V even higher) [77,85]. Moreover, the doubly anionic porphyrin ring favors a high oxidation state more than the mono-anionic corrin ring. Together, these two effects ensure that the Co(I) state is accessible in CoCor, whereas it is not observed for FePor [77].

As we have seen in this account, the use of the cobalamins as cofactors in the transferases and mutases is related to the unique properties of the Co–C bond, which is broken, either heterolytically or homolytically. Therefore, it was of considerable interest to compute the Co–C BDEs for various combinations of metal ions and ring systems, to understand whether the Co–C bond in corrins is special [77,85]. Interestingly, it was found that the homolytic metal–carbon BDE is 10 kJ/mol larger for CoCor than for FePor [77], showing that the Co–C bond is not particularly weak (although much weaker than an organic C–H bond).

However, this could in fact be a functional advantage: it is apparent that a bond that should supply radicals has to be fairly weak, to allow reversible cleavage, but it also needs to be stable enough to reform, in order to complete the catalytic cycle. In addition, the bond must be stable until it is needed. In particular, it must be stable against hydrolysis [133,134]. Such a notion was tested directly by computing the reaction energies of hydrolysis reactions for the various organometallic cofactors [77]. The Co–C bond was found to be 33–48 kJ/mol more resistant to hydrolysis than the Fe–C bond [77]. On the other hand, Ni displays even weaker Ni–C bonds than Fe [85]. This is somewhat unexpected, because such bonds have been postulated to occur in the coenzyme F430, but the Ni–C bond is so weak that the suggested homolytic mechanisms [135] can be ruled out [85,136].

We have also studied the corresponding heterolytic reactions, i.e. the transfer of a methyl group from the metal to various acceptors (e.g. a deprotonated homocysteine in MES) [77,85]. Our results showed that the M–C bond strength follows the trend Ni < Co < Fe, with differences of 10 and 80 kJ/mol, respectively. However, the reaction energies depend strongly on the methyl donor/acceptor, and it is therefore still possible that the methyl group binds directly to Ni in coenzyme F430 enzymes, provided that the donor is properly activated [85].

Altogether, these results clearly show how the cobalamin cofactor has been evolved to function as a reversible radical generator. The importance of the protein lies in further tuning the bond-dissociation reaction, substantially reducing the effective Co–C BDE as described above, aligning reactants, and securing reformation of the coenzyme after the reaction.

5. Concluding remarks

In this review, we have described how modern computational chemistry, in particular density functional methods, have brought forward our understanding of the cobalamin-dependent enzymes, exemplified by methionine synthase, glutamate mutase, and methylmalonyl coenzyme A mutase. The structure–function correlations of the cobalt-dependent cofactors have been explained in detail, both in realistic protein models and in relation to other alternative tetrapyrrole cofactors. The results are in excellent agreement with experimental data, but they go far beyond in terms of atomistic information. A clear picture has emerged for the design of cobalamin as capable of incorporating low-spin Co(I), Co(II), and Co(III) necessary for catalysis. The low-spin architecture ensures fast recombination of directed σ-radicals without spin crossover, something quite different from the design of heme cofactors, where spin crossover is needed for oxygen activation. The corrin ring thus serves as a framework for stabilizing these cobalt states, but not for specifically lowering the Co–C bond dissociation energy beyond its intrinsic value, as has previously been thought; this is instead the purpose of the proteins, which have evolved to provide a unique environment of electrostatic residues pulling the adenosyl radical away from corrin, thus bringing the Co(III) and Co(II) states close in energy in the mutases, and facilitating reversible radical formation. In methionine synthase, on the other hand, the protein residues are non-polar and maximize the rate of the polar S_N2 reaction. The reaction generates a Co(I) supernucleophile, which is likely to contain some Co(II) character, making this state more accessible for the transferases.

Acknowledgements

This research has been supported by grants from the Swedish Research Council and by computer resources of Lunarc at Lund University. K.P.J. acknowledges support from the Villum Kann-Rasmussen Foundation and from the Danish Center of Scientific Computing (DCSC).

References

[1] R.H. Abeles, D. Dolphin, Accounts Chem. Res. 9 (1976) 114.
[2] J.P. Glusker, Vitam. Horm. 50 (1995) 1.
[3] N. Shibata, J. Masuda, T. Tobimatsu, T. Toraya, K. Suto, Y. Morimoto, N. Yasuoka, Structure 7 (1999) 997.
[4] C.L. Drennan, S. Huang, J.T. Drummond, R.G. Matthews, M.L. Ludwig, Science 266 (1994) 1669.
[5] F. Mancia, N.H. Keep, A. Nakagawa, P.F. Leadlay, S. McSweeney, B. Rasmussen, P. Bösecke, O. Diat, P.R. Evans, Structure 4 (1996) 339.
[6] M.L. Ludwig, R.G. Matthews, Annu. Rev. Biochem. 66 (1997) 269.
[7] A. Coppen, C. Bolander-Gouaille, J. Psychopharm. 19 (2005) 59.
[8] E.N.G. Marsh, Bioorg. Chem. 28 (2000) 176.
[9] B.T. Golding, R.J. Anderson, S. Ashwell, C.H. Edwards, I. Garnett, F. Kroll, W. Buckel, in: B. Kräutler, D. Arigoni, B.T. Golding (Eds.), Vitamin B12 and the B12 Proteins, Wiley–VCH, Weinheim, 1998 (Chapter 12).
[10] B.M. Babior, T.J. Carty, R.H. Abeles, J. Biol. Chem. 249 (1974) 1689.
[11] T. Toraya, Cell. Mol. Life Sci. 57 (2000) 106.
[12] E.N.G. Marsh, C.L. Drennan, Curr. Opin. Chem. Biol. 5 (2001) 499.
[13] M.D. Waddington, R.G. Finke, J. Am. Chem. Soc. 115 (1993) 4629.
[14] R.G. Finke, in: B. Kräutler, D. Arigoni, B.T. Golding (Eds.), Vitamin B12 and the B12 Proteins, Wiley–VCH, Weinheim, 1998 (Chapter 25).
[15] R.G. Finke, B.P. Hay, Inorg. Chem. 23 (1984) 3041.
[16] K.L. Brown, X. Zou, J. Inorg. Biochem. 77 (1999) 185.
[17] T. Koenig, R.G. Finke, J. Am. Chem. Soc. 110 (1988) 2657.
[18] T.W. Koenig, B.P. Hay, R.G. Finke, Polyhedron 7 (1988) 1499.
[19] B.P. Hay, R.G. Finke, J. Am. Chem. Soc. 108 (1986) 4820.
[20] R. Padmakumar, R. Padmakumar, R. Banerjee, Biochemistry 36 (1997) 3713.
[21] T.W. Meier, N.H. Thomä, P.F. Leadlay, Biochemistry 35 (1996) 11791.
[22] S. Chowdhury, R. Banerjee, Biochemistry 39 (2000) 7998.
[23] S.S. Licht, C.C. Lawrence, J. Stubbe, Biochemistry 38 (1999) 1234.
[24] G.N. Schrauzer, R.J. Windgassen, J. Am. Chem. Soc. 88 (1966) 3738.
[25] K.L. Brown, S. Satyanarayana, J. Am. Chem. Soc. 114 (1992) 5674.
[26] D. Dodd, M.D. Johnson, B.L. Lockman, J. Am. Chem. Soc. 99 (1977) 3664.
[27] R.C. Stewart, L.G. Marzilli, J. Am. Chem. Soc. 100 (1978) 817.
[28] C. Tavagnacco, G. Balducci, G. Costa, K. Taschler, W. von Philipsborn, Helv. Chim. Acta 73 (1990) 1469.
[29] J.P. Charland, E. Zangrando, N. Bresciani-Pahor, L. Randaccio, L.G. Marzilli, Inorg. Chem. 32 (1993) 4256.
[30] L.G. Marzilli, P.J. Toscano, L. Randaccio, N. Bresciani-Pahor, M. Calligaris, J. Am. Chem. Soc. 101 (1979) 6754.
[31] H.A.O. Hill, J.M. Pratt, R.P.J. Williams, Chem. Ber. 5 (1969) 169.

[32] J.H. Grate, G.N. Schrauzer, J. Am. Chem. Soc. 101 (1979) 4601.
[33] J. Halpern, Science 227 (1985) 869.
[34] L.M. Hansen, A. Derecskei-Kovacs, D.S. Marynick, J. Mol. Struct. THEOCHEM 431 (1998) 53.
[35] K.P. Jensen, K.V. Mikkelsen, Inorg. Chim. Acta 323 (2001) 5.
[36] L. Randaccio, M. Furlan, S. Geremia, M. Slouf, I. Srnova, D. Toffoli, Inorg. Chem. 39 (2000) 3403.
[37] C. Michael Elliott, E. Herschenhart, R.G. Finke, B.L. Smith, J. Am. Chem. Soc. 103 (1981) 5558.
[38] H.M. Marques, K.L. Brown, Coord. Chem. Rev. 190–192 (1999) 127.
[39] N. Bresciani-Pahor, M. Forcolin, L.G. Marzilli, L. Randaccio, M.F. Summers, P.J. Toscano, Coord. Chem. Rev. 63 (1985) 1.
[40] S. Dong, R. Padmakumar, R. Banerjee, T.G. Spiro, J. Am. Chem. Soc. 121. (1999).
[41] M.D. Vlasie, R. Banerjee, J. Am. Chem. Soc. 125 (2003) 5431.
[42] F. Mancia, P.R. Evans, Structure 6 (1998) 711.
[43] R. Banerjee, Chem. Biol. 4 (1997) 175.
[44] M. Tollinger, R. Konrat, B.H. Hilbert, E.N.G. Marsh, B. Kräutler, Structure 6 (1998) 1021.
[45] E. Scheuring, R. Padmakumar, R. Banerjee, M.R. Chance, J. Am. Chem. Soc. 119 (1997) 12192.
[46] K.P. Jensen, U. Ryde, J. Mol. Struct. THEOCHEM 585 (2002) 239.
[47] R. Reitzer, K. Gruber, G. Jogl, U.G. Wagner, H. Bothe, W. Buckel, C. Kratky, Structure 7 (1999) 891.
[48] K. Gruber, R. Reitzer, C. Kratky, Angew. Chem. Int. Ed. 40 (2001) 3377.
[49] D.J.A. De Ridder, E. Zangrando, H.-B. Burgi, J. Mol. Struct. 374 (1996) 63.
[50] B. Krautler, W. Keller, C. Kratky, J. Am. Chem. Soc. 111 (1989) 8936.
[51] B.P. Hay, R.G. Finke, J. Am. Chem. Soc. 109 (1987) 8012.
[52] F. Champloy, G. Jogl, R. Reitzer, W. Buckel, H. Bothe, B. Beatrix, G. Broeker, A. Michalowicz, W. Meyer-Klaucke, C. Kratky, J. Am. Chem. Soc. 121 (1999) 11780.
[53] J.S. Trommel, K. Warncke, L.G. Marzilli, J. Am. Chem. Soc. 123 (2001) 3358.
[54] E.N.G. Marsh, D.E. Holloway, H.-P. Chen, in: B. Kräutler, D. Arigoni, B.T. Golding (Eds.), Vitamin B12 and the B12 Proteins, Wiley–VCH, Weinheim, 1998 (Chapter 16).
[55] R. Banerjee, Chem. Rev. 103 (2003) 2083.
[56] M. Vlasie, S. Chowdhury, R. Banerjee, J. Biol. Chem. 277 (2002) 18523.
[57] H.-P. Chen, F.-D. Lung, C.-C. Yeh, H.-L. Chen, S.-H. Wu, Bioorg. Med. Chem. 12 (2004) 577.
[58] J.S. Dorweiler, R.G. Finke, R.G. Matthews, Biochemistry 42 (2003) 14653.
[59] K. Nilsson, U. Ryde, J. Am. Chem. Soc. 125 (2003) 14232.
[60] D.W. Christianson, W.N. Lipscomb, J. Am. Chem. Soc. 107 (1985) 2682.
[61] J.P. McNamara, M. Sundararajan, I.H. Hillier, J. Ge, A. Campbell, C. Morgado, J. Comput. Chem. 27 (2006) 1307.
[62] D.M. Smith, B.T. Golding, L. Radom, J. Am. Chem. Soc. 121 (1999) 1383.
[63] S.D. Wetmore, D.M. Smith, L. Radom, Chem. Bio. Chem. 12 (2001) 919.
[64] S.D. Wetmore, D.M. Smith, L. Radom, J. Am. Chem. Soc. 123 (2001) 8678.
[65] M.J. Loferer, B.M. Webb, G.H. Grant, K.R. Liedl, J. Am. Chem. Soc. 125 (2003) 1072.
[66] K.P. Jensen, U. Ryde, J. Phys. Chem. B 107 (2003) 7539.
[67] T. Andruniow, M.Z. Zgierski, P.M. Kozlowski, J. Phys. Chem. B 104 (2000) 10921.
[68] K.P. Jensen, S.P.A. Sauer, T. Liljefors, P.-O. Norrby, Organometallics 20 (2001) 550.
[69] T. Andruniow, M.Z. Zgierski, P.M. Kozlowski, Chem. Phys. Lett. 331 (2000) 509.
[70] N. Dölker, F. Maseras, A. Lledos, J. Phys. Chem. B 105 (2001) 7564.
[71] P.M. Kozlowski, Curr. Opin. Chem. Biol. 5 (2001) 736.
[72] T. Andruniow, M.Z. Zgierski, P.M. Kozlowski, J. Chem. Phys. 115 (2001) 7522.
[73] A. Dybala-Defratyka, P. Paneth, J. Inorg. Biochem. 86 (2001) 681.
[74] T. Andruniow, M.Z. Zgierski, P.M. Kozlowski, J. Am. Chem. Soc. 123 (2001) 2679.
[75] M. Jaworska, P. Lodowski, J. Mol. Struct. THEOCHEM 631 (2003) 209.
[76] E.Z. Kurmaev, A. Moewes, L. Ouyang, L. Randaccio, P. Rulis, W.Y. Ching, M. Bach, M. Neumann, Europhys. Lett. 62 (2003) 582.
[77] K.P. Jensen, U. Ryde, Chem. Bio. Chem. 4 (2003) 413.
[78] K.P. Jensen, U. Ryde, J. Am. Chem. Soc. 125 (2003) 13970.
[79] N. Dolker, F. Maseras, A. Lledos, J. Phys. Chem. B 107 (2003) 306.
[80] N. Dolker, F. Maseras, P.E.M. Siegbahn, Chem. Phys. Lett. 386 (2004) 174.
[81] M. Freindorf, P.M. Kozlowski, J. Am. Chem. Soc. 126 (2004) 1928.
[82] P.M. Kozlowski, M.Z. Zgierski, J. Phys. Chem. B 108 (2004) 14163.
[83] T.A. Stich, N.R. Buan, T.C. Brunold, J. Am. Chem. Soc. 126 (2004) 9735.
[84] K.P. Jensen, U. Ryde, J. Am. Chem. Soc. 127 (2005) 9117.
[85] K.P. Jensen, U. Ryde, J. Porph. Phtalocyan. 9 (2005) 581.
[86] M.D. Liptak, T.C. Brunold, J. Am. Chem. Soc. 128 (2006) 9144.
[87] J. Kuta, S. Patchkovskii, M.Z. Zgierski, P.M. Kozlowski, J. Comput. Chem. 27 (2006) 1429.
[88] P.M. Kozlowski, J. Kuta, W. Galezowski, J. Phys. Chem. B 111 (2007) 7638.
[89] C. Rovira, P.M. Kozlowski, J. Phys. Chem. B 111 (2007) 3251.
[90] P.K. Sharma, Z.T. Chu, M.H.M. Olsson, A. Warshel, Proc. Natl. Acad. Sci. U.S.A. 104 (2007) 9661.
[91] D.V. Khoroshun, K. Warncke, S.-C. Ke, D.G. Musaev, K. Morokuma, J. Am. Chem. Soc. 125 (2003) 570.
[92] R.A. Kwiecien, I.V. Khavrutskii, D.G. Musaev, K. Morokuma, R. Banerjee, P. Paneth, J. Am. Chem. Soc. 128 (2006) 1287.
[93] A.D. Becke, J. Chem. Phys. 98 (1993) 5648.
[94] F. Jensen, Introduction to Computational Chemistry, John Wiley & Sons, 1999.
[95] F. Himo, P.E.M. Siegbahn, Chem. Rev. 103 (2003) 2421.
[96] G. Frenking, N. Frohlich, Chem. Rev. 100 (2000) 717.
[97] P.E.M. Siegbahn, M.R.A. Blomberg, Chem. Rev. 100 (2000) 421.
[98] T. Ziegler, Chem. Rev. 91 (1991) 651.
[99] T. Ziegler, Can. J. Chem. 73 (1995) 743.
[100] P.E.M. Siegbahn, M.R.A. Blomberg, Annu. Rev. Phys. Chem. 50 (1999) 221.
[101] A.D. Becke, Phys. Rev. A 38 (1988) 3098.
[102] J.P. Perdew, Phys. Rev. B 33 (1986) 8822.
[103] F. Neese, J. Biol. Inorg. Chem. 11 (2006) 702.
[104] J.F. Harrison, Chem. Rev. 100 (2000) 679.
[105] K.P. Jensen, B.O. Roos, U. Ryde, J. Chem. Phys. 126 (2007) 014103.
[106] K.L. Brown, S. Cheng, X. Zou, J. Li, G. Chen, E.J. Valente, J.D. Zubkowski, H.M. Marques, Biochemistry 37 (1998) 9704.
[107] J. Li, G. Schreckenbach, T. Ziegler, J. Am. Chem. Soc. 117 (1995) 486.
[108] R.K. Birke, Q. Huang, T. Spataru, D.K. Gosser Jr., J. Am. Chem. Soc. 128 (2006) 1922.
[109] T. Spataru, R.L. Birke, J. Phys. Chem. A 110 (2006) 8599.
[110] W. Galezowski, J. Kuta, P.M. Kozlowski, J. Phys. Chem. B 112 (2008) 3177.
[111] M.D. Liptak, A.S. Fleischhacker, R.G. Matthews, T.C. Brunold, Biochemistry 46 (2007) 8024.
[112] M.D. Wirt, I. Sagi, E. Chen, S.M. Frisbie, R. Lee, M.R. Chance, J. Am. Chem. Soc. 113 (1991) 5299.
[113] K.P. Jensen, J. Phys. Chem. B 109 (2005) 10505.
[114] N. Dölker, A. Morreale, F. Maseras, J. Biol. Inorg. Chem. 10 (2005) 509.
[115] S.J. Weiner, P.A. Kollman, D.T. Nguyen, D.A. Case, J. Comput. Chem. 7 (1986) 230.
[116] S.J. Weiner, P.A. Kollman, D.A. Case, U.C. Singh, C. Ghio, G. Alagona, S. Profeta Jr., P. Weiner, J. Am. Chem. Soc. 106 (1984) 765.
[117] H.M. Marques, B. Ngoma, T.J. Egan, K.L. Brown, J. Mol. Struct. THEOCHEM 561 (2001) 71.
[118] U. Ryde, J. Comput.-Aided Mol. Design. 10 (1996) 153.
[119] U. Ryde, M.H.M. Olsson, Int. J. Quant. Chem. 81 (2001) 335.
[120] F. Mancia, G.A. Smith, P.R. Evans, Biochemistry 38 (1999) 7999.
[121] K. Nilsson, D. Lecerof, E. Sigfridsson, U. Ryde, Acta Crystallogr. D 59 (2003) 274.
[122] C. Kratky, K. Gruber, in: A. Messerschmidt, R. Huber, K. Wieghardt, T. Poulos (Eds.), Handbook of Metalloproteins, Wiley, Chichester, 2001, p. 983.
[123] K. Gruber, C. Kratky, Curr. Opin. Struct. Biol. 6 (2002) 598.
[124] A. Warshel, Computer Modeling of Chemical Reactions in Enzymes and Solutions, Wiley, New York, 1991.
[125] J. Åqvist, A. Warshel, Chem. Rev 93 (1993) 2523.
[126] A.M. Stolzenberg, M.T. Stershic, J. Am. Chem. Soc. 110 (1988) 6391.
[127] R.H. Holm, P. Kennepohl, E.I. Solomon, Chem. Rev. 96 (1996) 2239.
[128] K.P. Jensen, U. Ryde, Mol. Phys. 13 (2003) 2003.
[129] K.P. Jensen, U. Ryde, J. Biol. Chem. 279 (2004) 14561.
[130] E. Sigfridsson, M.H.M. Olsson, U. Ryde, J. Phys. Chem. B 105 (2001) 5546.
[131] K.P. Jensen, J. Inorg. Biochem. 100 (2006) 1436.
[132] J.G. Stark, H.G. Wallace, Chemistry Data Book, John Murray, London, 1982.
[133] M.P. Jensen, J. Halpern, J. Am. Chem. Soc. 121 (1999) 2181.
[134] J.M. Pratt, Pure Appl. Chem. 65 (1993) 1513.
[135] W.G. Grabarse, F. Mahlert, S. Shima, R.K. Thauer, U. Ermler, J. Mol. Biol. 303 (2000) 329.
[136] V. Pelmenschikov, P.E.M. Siegbahn, J. Biol. Inorg. Chem. 8 (2003) 653.